Charles University in Prague

Faculty of Mathematics and Physics

Abstract of Doctoral Thesis

David Hanslian

Wind data analysis

Department of Meteorology and Environment Protection
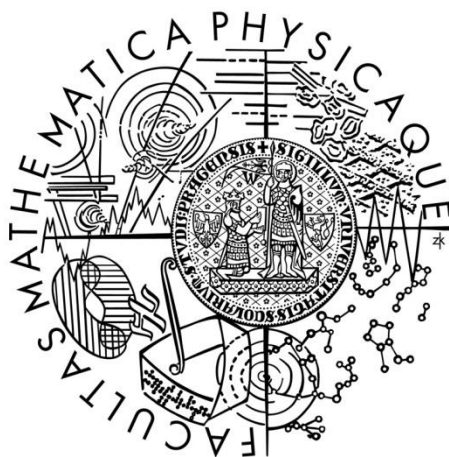
Supervisor: doc. RNDr. Jaroslava Kalvová, CSc.

Branch of study: 4F8 Meteorology and Climatology

Prague 2014

Univerzita Karlova v Praze

Matematicko-fyzikální fakulta

Autoreferát dizertační práce

Mgr. David Hanslian

Analýza výsledků měření větru

Katedra meteorologie a ochrany prostředí

Vedoucí disertační práce: doc. RNDr. Jaroslava Kalvová, CSc.

Studijní obor: 4F8 Meteorologie a klimatologie

Praha 2014

Doktorand:
Mgr. David Hanslian

Školitel:
doc. RNDr. Jaroslava Kalvová, CSc.

Školící pracoviště:
Katedra meteorologie a ochrany prostředí MFF UK
V Holešovičkách 2, 180 00 Praha 8

Oponenti:
RNDr. Vít Květoň, CSc.
Český hydrometeorologický ústav
Na Šabatce 17
140 00 Praha 4

RNDr. Radan Huth, DrSc.
Přírodovědecká fakulta UK
Katedra fyzické geografie a geoekologie
Albertov 6
128 43 Praha 2

<u>Contents</u>

1. Introduction

With a little hyperbole it can be claimed, that wind is a meteorological variable that "makes troubles". At first, it is not easy to obtain a precise measurement of wind conditions. The common sources of measurement errors are low quality or poor design of measuring equipment, erroneous measurement set-up, insufficient maintenance of sensors or adverse external conditions (e.g. icing). Another challenge is the measurement siting. It is often difficult to avoid significant effects of nearby objects on the measured wind conditions. Finally, the wind data analysis and application are complicated by the vector nature of wind variable and its high temporal and spatial variability.

The presented thesis attempts to analyze and mitigate some of these issues. Its first part (Chapter 2) is mainly focused on the undesirable effects of anemometer siting, which can affect the measured wind data. The second part of the thesis (Chapter 3) deals with the extension (or completion) of wind data series by measure-correlate-predict (MCP) methods. The final part (Chapter 4) analyses the wind conditions over the Czech Republic and the calculation of the wind map of the Czech Republic is described here.

## *2. Effects of anemometer siting on measured wind data*

The requirements on wind data depend on the purpose for which they are used. While some applications require, in absolute terms, high-accuracy measurement of wind speed, other applications can accept some uncertainty in this aspect. Some applications need wind data with high temporal resolution, the other can manage with few measurements per day. Some applications need the precise wind directions measurements, the other do not...

Similarly, the requirements on anemometer siting also depend on for which purpose are the data used for. For example, some microclimatic or air quality applications may require wind data from the forest clearings or from the sites inside urban areas, sheltered by nearby buildings. The same positions are, however, unacceptable for many other applications, which require measurement of "regionally representative" wind conditions affected by local obstacles as little as possible. In these cases the local effects on the observed wind conditions are considered as a source of errors and the aim is to avoid them or to quantify them in order to be able to correct the affected data. But the application, for which the data are used, should again be taken into account to determine the acceptable extent of siting effects or their uncertainty. The requirements for basic meteorological measurements (WMO, 2008, part I/5), that must also consider practical constraints of wind measurements at meteorological stations, are much less demanding compared with rigorous requirements for specialized wind mast measurements in wind energy (IEA, 1999, MEASNET, 2008).

2.1 Small-scale effects

The measured wind conditions can be surprisingly strongly affected by wind flow deformation induced by poor anemometer design and by objects close to the anemometer. These issues are closely described in IEA (1999) recommendations.

An inevitable obstacle affecting mast measurements of wind profile is the wind mast itself. This topic has been investigated in multiple studies (e.g. Stickland et al., 2012, Lindelöw et al., 2010, Orlando et al., 2011 or Farrugia & Sant, 2013). The wind flow is obviously most disturbed at the wake of the wind mast, but the entire wind field around wind mast is affected. The wind speed in upwind direction tends to be reduced, whereas on the sides of the mast the wind speed increases (Figure 1). To reduce these effects (except the wake effect) under 1 % of ambient wind speed, the anemometer should be positioned at least approximately 6 mast diameters out of the mast; for reduction of these effects under 0.5 %, the distance required is 8.5 mast diameters (IEA, 1999). The effects around porous lattice tower are relatively lower. To avoid the effects of wake behind the mast, installation of multiple anemometers in different direction is recommended (WMO, 2008, part II/5.3.3). Example of results of wind mast measurement designed this way (Figure 2) is shown at Figure 3.
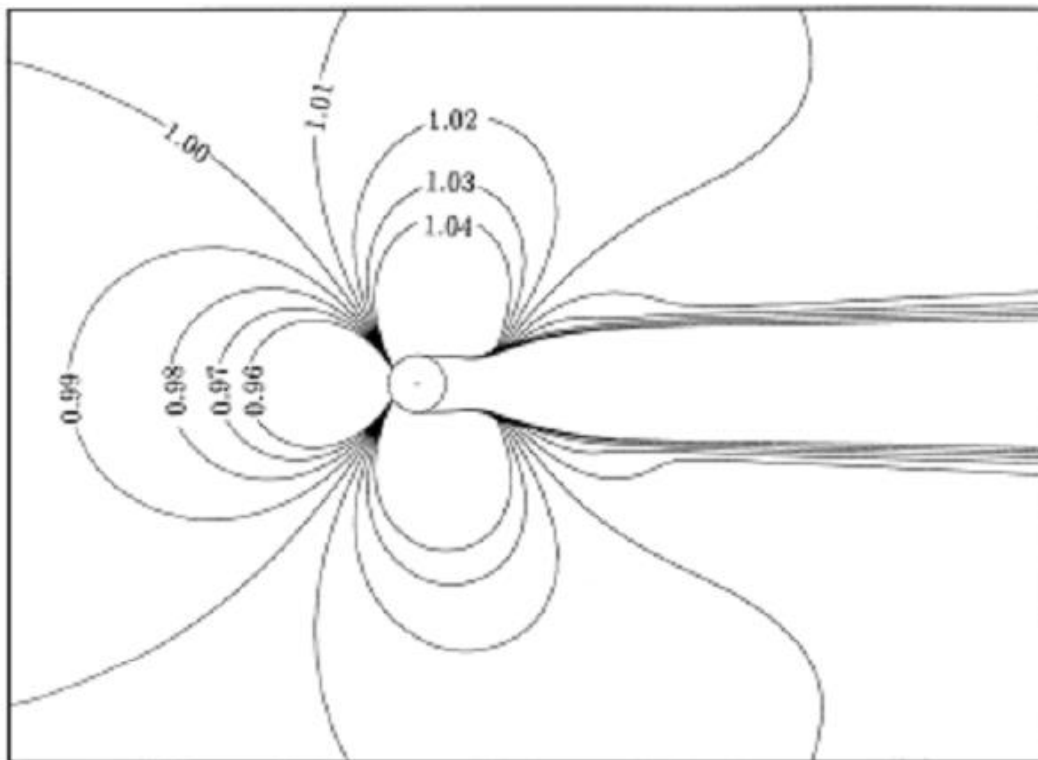
Figure 1 *Simulated field of average wind speed near the tubular wind mast (wind flows from the left). The wind speed is shown in relative number against the undisturbed wind. Source: IEA (1999)*

Figure 2 *Wind mast measurement analyzed at Figure 3. The anemometers are positioned 1.53 m (7.5 mast diameters) out of the wind mast of diameter 20.3 cm.*
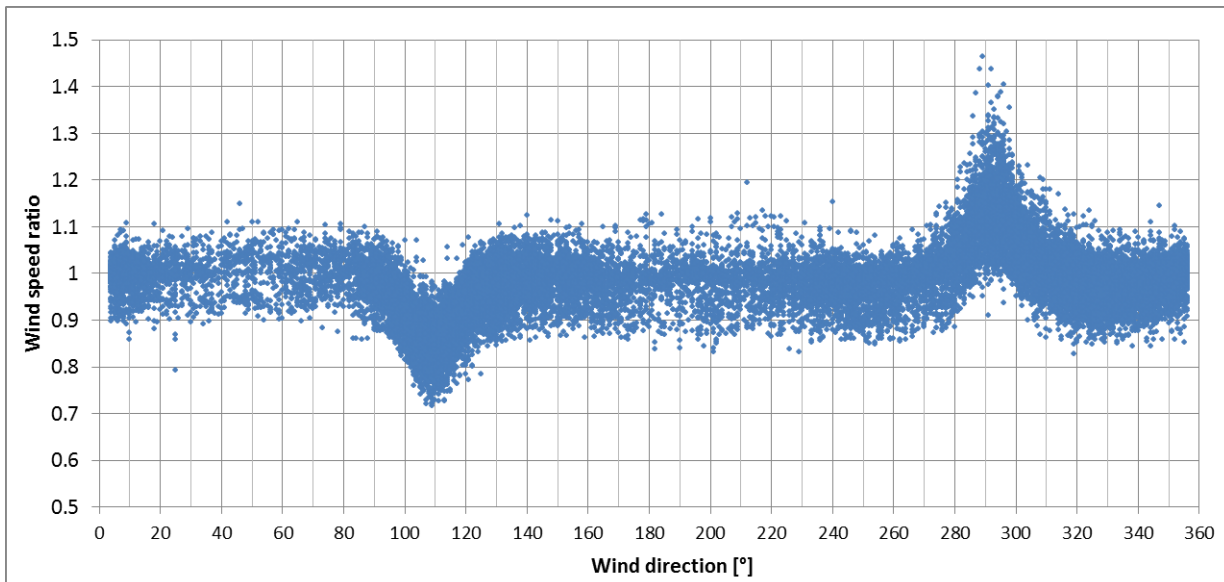
Figure 3 *Ratios between the individual recorded wind speeds at sensors positioned at the opposite sided of wind mast shown at Figure 2 (1 year of measurement). Only the records with average wind speed above 2.5 m/s are considered. The shading effect of wind mast is obvious, the effects in other directions are less pronounced.*

The measured wind can be also affected by any other kind of object close to the recommend the minimum distance of anemometer from the lightning rod at least 50 of lightning rod diameters and the minimum vertical distance above the horizontal boom at least 12 of boom diameters (see also an example at Figure 4 and Figure 5).anemometer, such as antennae, other sensors etc. Even very tiny objects, such as lightning rods or wires, can influence the measured data if they are close enough. Also horizontal booms or objects above or behind anemometers can influence the wind flow. For illustration, the rigorous wind energy standards (IEA, 1999, MEASNET, 2008)

Figure 4 *Wind mast measurement analyzed at* *Figure 5*, *view from southwest. The top anemometer (40 m) is positioned approximately 40 cm above the mast top and 20 cm besides the lightning rod. The anemometer 39.5 m (at left) is 1.7 m besides the mast top. The anemometer 24 m (not shown here) is positioned analogously as anemometer 39.5 m. The mast diameter is 17 cm and the lightning rod diameter is 0.9 cm, so the 40 m sensor is only 3 mast diameters above the mast top and 22 diameters of lightning rod besides it, both markedly under* *IEA (2008)* *recommendations.*
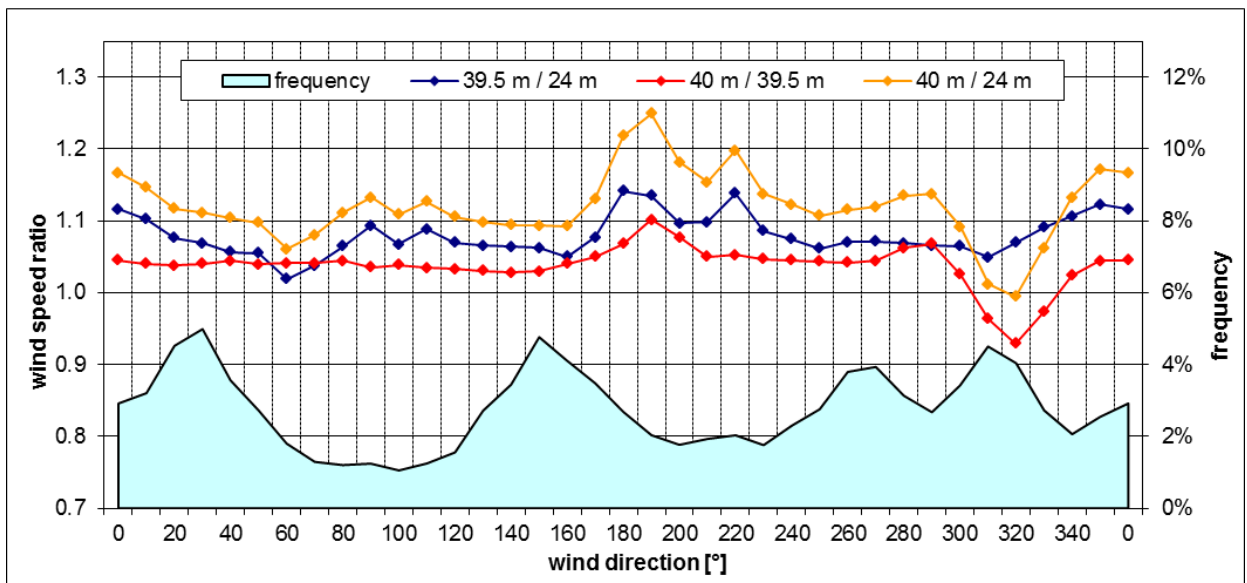
Figure 5 *Ratios between average wind speeds (1 year of measurement) at anemometers at heights 24 m, 39.5 m and 40 m (see* *Figure 4*). *The shading of the top (40 m) anemometer by lightning rod (directions 310 – 330 °) is stronger than shading of the other anemometers by wind mast (directions 180 – 190°). The wind speed measured at 40 m anemometer is much higher, than at 39.5 m: detailed wind data analysis revealed, that the wind speed at 40 m is probably overestimated by 2 % of wind speed by wind speed-up above the mast top, the rest of the difference between 39.5 m a 40 m can be explained by other factors.*

2.2 Wind measurements above buildings

A common practice of wind measurement at manned meteorological stations is positioning the anemometer above the building. The WMO (2008) standard allows such position if the anemometer is at height at least one building width above the roof. Such position ensures, that the measurement is outside the zone of perturbed wind, which develops close above the roof. However, wind measured this way is affected by wind speed-up above the building.

It is surprising, how little attention is paid to this issue. Despite the large number of studies of wind flow around buildings, the only article found by the author of this thesis, that attempts to quantify the effects of this wind speed-up on anemometer readings, was published by Landberg (2000). This study is based on the experimental results and provides a simple guide, how to estimate the magnitude of speed-up by simplified WAsP model.

Figure 6 *The typical manned weather station Kuchařovice. The observed wind climate is affected by the anemometer position above the rooftop, by the forest behind (its potentially strong effect is limited by low frequency of wind direction from the forest), by near-by trees, a wind mast and a parallel anemometer.*
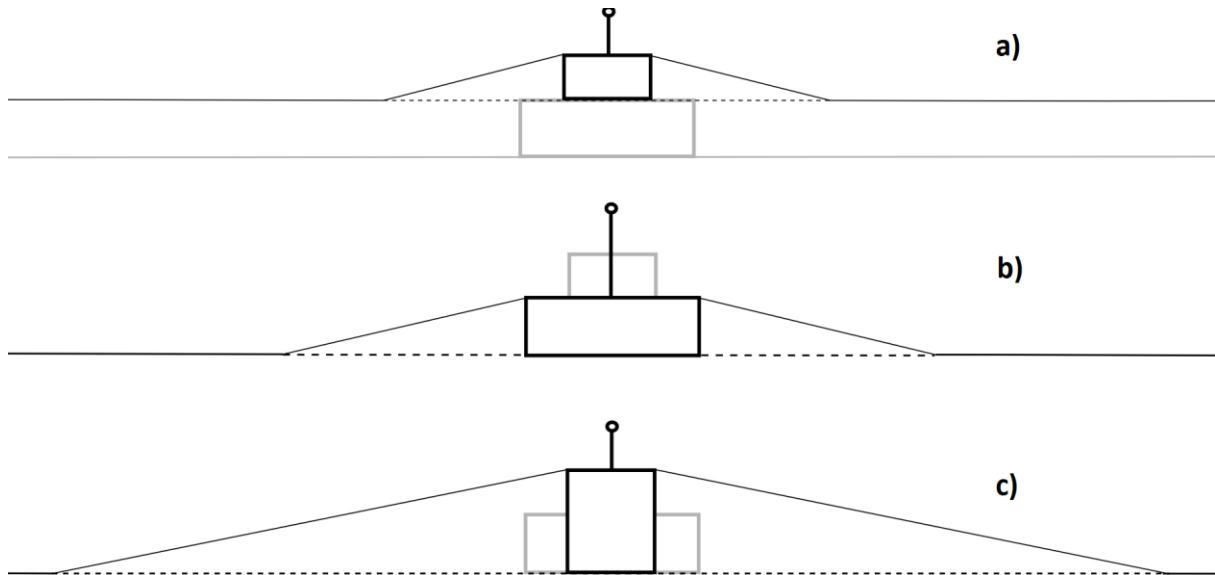
Figure 7 A schematic drawing of three approaches, how to approximate the weather station at Figure 6 by orographic elevation.

Height above roof (above ground)	a) only upper part	b) only lower part	c) entire height
2 m (9 m)	32.2 %	17.1 %	58.4 %
3 m (10 m)	**22.2 %**	**14.5 %**	**42.1 %**
4 m (11 m)	16.7 %	12.5 %	33.2 %
5 m (12 m)	13.1 %	10.9 %	27.4 %
7 m (14 m)	8.7 %	8.4 %	20.1 %
10 m (17 m)	5.2 %	6.0 %	14.0 %

Table 1 Simulated speed-up over the building of typical weather station depicted at Figure 6 and Figure 7.

Following the recommendation of Landberg (2000), wind speed-up of wind measurement above the typical Czech meteorological station (Figure 6) was estimated. According to it, the building should be represented in WAsP model as a hill with the same height and slope 1:5. The pyramidal shape of the building was represented by three alternative approaches (Figure 7), where only the upper part (a), only the lower part (b) or the entire height (c) of the building was considered.

The results (Table 1) show, that even in the case of the conservative approaches a) or b), the estimated speed-up is far from negligible. The overestimation of measured wind speed at these stations can be probably as high as around 20 %! In real cases the effect will be probably reduced or partially compensated by the occurrence of obstacles around these stations and the applied approach must be considered as only approximate. Nevertheless, the result still indicates, that the speed-up is much more serious issue than has been commonly thought.

Similar effects occur when the anemometer is located above the top of other objects, such as tall wind mast or telecommunication mast. Perrin et al. (2007) calculated, that speed-up about 1 % can be expected above the top of tubular hollow wind mast even at height of 5 its diameters. A strict IEA (2008) recommendation expect the 0.5 % speed-up at height of 8.5 its diameters. This speed-up is also the most probable explanation of the major part of the difference between the measured wind speeds at sensors 39.5 m and 40 m at Figure 5.

2.3 Effects of surrounding obstacles

The effect of local obstacles can strongly change the wind conditions at a measurement site. To estimate the magnitude of these effects, high-resolution numerical or physical simulation can be performed. This is, however, not practical in most cases. Alternatively, simplified approaches may be applied. Three typical cases can be specified:

1) The wind measurement is located at generally open site with only limited number of well defined obstacles (e.g. the measurements on airports or in the agricultural land with windbreaks). In that case the effects of the individual obstacles can be estimated. The well known approximate calculation of the wake effect behind the infinitely long obstacle was performed by Perera (1981) and incorporated into the widely used model WAsP (Troen & Petersen, 1989 - Figure 8).
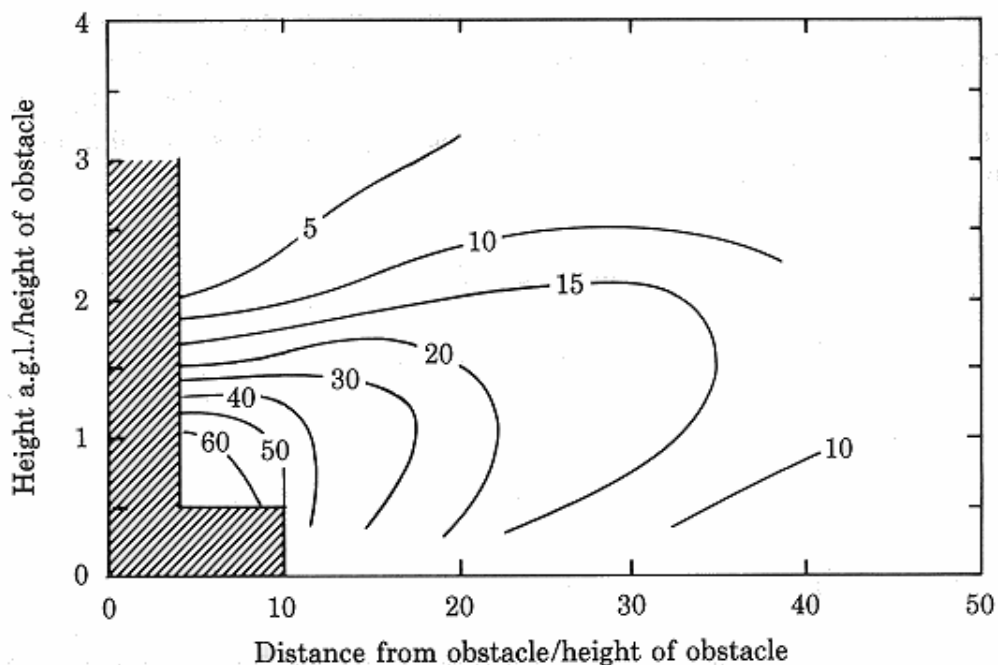
Figure 8 *The average shading effect (in percent of ambient wind speed) behind non-porous infinitely long two-dimensional obstacle according to the study of Perera (1981). In the shaded area the effects strongly depends on the obstacle shape and they cannot be generalized. Source:* Troen & Petersen (1989).

It can be observed, that behind the non-porous obstacle more than 10 % reduction of wind speed can be expected even at the height of two obstacle heights or at the distance of 40 obstacle heights. In the minimum recommended distance by WMO (2008) standard, which is 10 obstacle heights, the wind speed reduction can be as high as 50 % (!) Much larger distance is therefore recommended in wind energy practice (e.g. Brower et al., 2012). The wind speed reduction is lower for porous obstacles (Troen & Petersen, 1989) and for obstacles of finite widths (Brunskill & Lubitz, 2012).

2) The "obstacles" form a field of large number of elements of similar height and density. This is typically the case of forest, but the effects of homogeneous urban areas or many kinds of vegetation formation (vineyards, plantations, bushes etc.) can be similar. The simplified model of the wind flow above forest assumes that the vertical wind profile is displaced upwards by a *displacement height*. This height (and the roughness length of the displaced surface) depends on the height of the canopy and on its density. In the case of typical forest it equals about ¾ of the canopy height (Raupach, 1994, Verhoef et al., 1997). This theory, however, effectively works only high above the forest (the height of 3 forest heights above surface is mostly mentioned, e.g. Harman & Finigan, 2007 or Foken, 2008) and it increases with increasing distance between individual elements (Oke, 2008), (Figure 9). Below this height the turbulence intensity is increased and wind conditions are hardly predictable; this areas is called as *roughness sublayer*. As a result, if the accurate regionally representative wind information is desired, then wind measurement inside forests (or urban areas) and even up to some height above their tops should be avoided, because such data are very difficult to correct reliably.
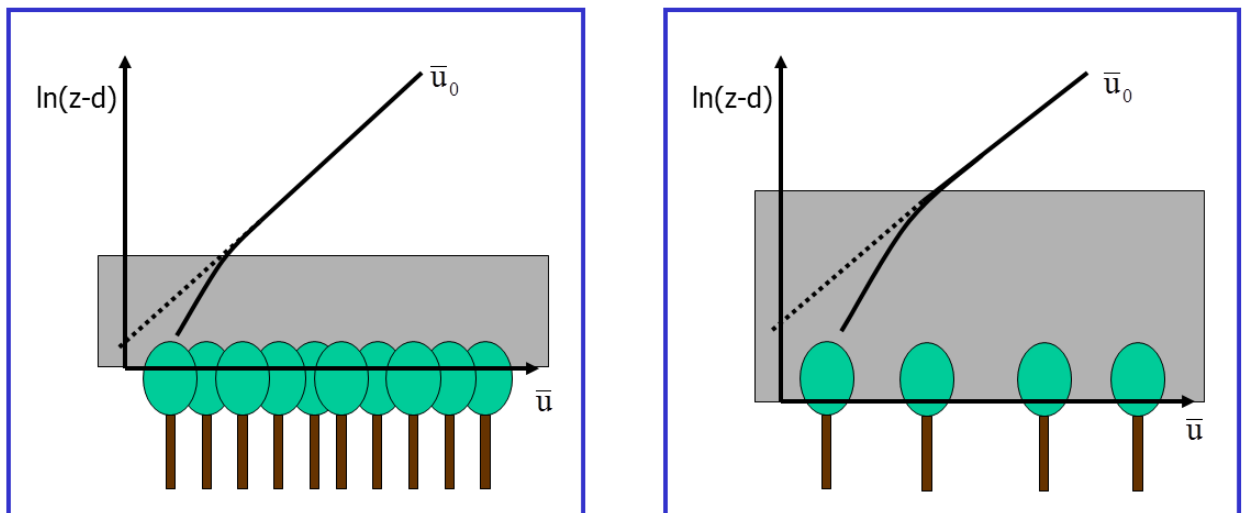
Figure 9 *Schematic drawing of vertical wind profile over dense and sparse forest. The sparser forest of the same vegetation height lowers the displacement height, however the roughness length rather increases and the roughness sublayer (shaded) is much thicker. Source: Dellwik et al. (2004)*

3) The configuration of obstacles is complex and cannot be described either as a group of simple individual obstacle or as a homogeneous field of elements. In this case only a simplified estimation of the wake or the spatial effects can be done and a strong uncertainty can hardly be avoided.

3. Measure-correlate-predict methods

3.1 Overview of MCP methods

The measure-correlate-predict (MCP) methods are used to simulate the wind conditions at a *target* wind data series in the time period when the measured data are not available. The simulation is based on another (*reference*) wind data series, which is homogeneous and covers the period with the target data available as well as the period, for which the missing target data are simulated. The most typical application of MCP is the extension of a short-term wind data from a temporary measuring campaign to the long-term wind conditions at the target site. In a more general sense, the MCP methods can be applied for other tasks, such as the correction of gaps in the target series or the estimation of wind conditions in specific occasions or periods.

The minimal length of the "training period", when the concurrent data from both sites are analyzed, depends on the closeness of the relationship between the series, on the applied methods and on the required accuracy of the result. For the typical application, the reference series is obtained at another location or extracted from reanalysis, so that the data are not closely correlated. In such case one full year of training data is recommended, in order to cover all seasons and all usual weather patterns.

The simplest MCP methods are the *methods of ratios*. They are based on the assumption that the wind speed basically behaves proportionally. This means that the ratio between the wind speed at the reference and target sites as well as the ratio between the wind speed in the training and long-term periods are constant. Then the average wind speed at the target series in the simulated period is calculated as

$$\bar{v}_c^d = \bar{v}_r^d * \frac{\bar{v}_c^t}{\bar{v}_r^t} \tag{1}$$

where $\bar{v}_r^d$ is the average wind speed of the reference series in the simulated period, $\bar{v}_c^t$ is the average wind speed of the target series in the training period etc.

This method can be also applied to other characteristics, e.g. to the parameters of Weibull distribution (*Weibull scale method* – Clive, 2008). A similar approach is used for calculation of so-called *wind indices*, which express the ratio of the average wind speed

or wind energy production of a given time period, such as individual months or years, against the long-term average (e.g. the BDB-index; www.enveco.de).

The ratios of average wind speeds can be also applied to the individual wind speed records, thus creating the artificial wind data series. If the ratio between the average wind speeds at target and reference sites is applied to the reference data, then the artificial wind data series can be constructed (e.g. Anderson, 2004):

$$v_c(T^d) = v_r(T^d) * \frac{\bar{v}_c^t}{\bar{v}_r^t} \tag{2}$$

where $v_c(T^d)$ a $v_r(T^d)$ represent the wind speed of the target and reference series at the time record T^d of the simulated period. This approach, however, does not simulate the wind speed distribution correctly.

The correct simulation of the wind speed distribution can be achieved by the calculation of the ratio between the average wind speeds of the simulated and training periods at the reference series and its application to the target data (*Windiness factor method* of King & Hurley, 2004). The simulated data cannot be matched to the individual time records of the simulated period, so they are labeled as T^x:

$$v_c(T^x) = v_c(T^d) * \frac{\bar{v}_r^d}{\bar{v}_r^t} \tag{3}$$

More elaborate kinds of the relationship between the reference and target data are employed in the other methods. Most common is the application of first-order *linear regression*:

$$v_c(T^d) = a * v_r(T^d) + b \tag{4}$$

To simulate the wind speed distribution, the linear regression must be supplemented by the simulation of residuals (e.g. EMD International A/S, 2008).

Various alternative regression approaches have been developed, such as the *SpeedSort* or *DynaSort* methods (King & Hurley (2005, in Carta et al., 2013) or *Variance ratio method* (5) (Rogers et al., 2005):

$$v_c(T^d) = \frac{s_c^t}{s_r^t} * v_r(T^d) + \left[\bar{v}_c^t - \left(\frac{s_c^t}{s_r^t} \right) \bar{v}_r^t \right] \tag{5}$$

For most methods the simulation can be further improved by classification of the data into groups (bins), that represent typical patterns of relationships between the data. Most common is grouping the data by the wind direction at the reference site, typically to 12 or 36 directional sectors. The data can be grouped also by e.g. the daytime, season, atmospheric stability or weather class.

All above mentioned methods are only focused on the simulation of the wind speed. To simulate the wind direction, a separate method must be applied. A functional

relationship between the wind directions (e.g. Riedel et al., 2001 (in Carta et al., 2013)) or the *veer correction* (King & Hurley, 2005 (in Carta et al., 2013)) can be employed (veer is defined as the difference between wind directions at the target and reference series). Disadvantage of these approaches is the fact, that the joint relationship between the wind speed and wind direction is not preserved, so that the directional distribution of the wind speed cannot be simulated this way.

Several methods apply grouping the data into bins by the wind speed at the reference site. The relation between the target and reference wind speed is calculated individually for each wind speed bin, which allows simulation of the target wind speed distribution. If the binning is performed jointly by the wind speed and wind direction, which is the most common approach, then these methods are called as *matrix methods* (e.g. Mortimer, 1994 (in Rogers et al., 2005), EMD International A/S, 2008). The wind direction can be simulated similarly (EMD International A/S, 2008).

The title "matrix method" is also used for another class of methods, which are based on the identification of <u>joint probabilities</u> $p^t(k_r, k_c)$ of bins defined both by the reference and by target series. Bins can be determined by wind speed, by wind direction, by other factors or by combination of them. It is calculated, how does the probability of occurrence of the individual bins change in response of the change of $\frac{p^d(k_r)}{p^t(k_r)}$ occurrence of involved bins at the reference site between the training and simulated period:

$$p^d(k_c) = \sum_{k_r=1}^{N_{kr}} \left[p^t(k_r, k_c) * \frac{p^d(k_r)}{p^t(k_r)} \right] \tag{6}$$

where $p^d(k_c)$ is the probability of occurrence of bin k_c defined by the target data in simulated period. The definition of bins k_c determines the resolution of the result, so that if the target data are binned by wind speed, then the wind speed distribution is simulated; if they are binned by wind direction, then the wind rose is simulated. If the target data are binned both by wind speed and wind direction (Salmon & Walmsley, 1999, García-Rojo, 2004), then the distribution of both variables is simulated, including their joint relationship.

The average wind speed can be simply derived from the distribution of the wind speed bins at target series or it can be calculated individually each bin k_c. Such approach was applied (differently) by Harstveit (2004, in Carta et al., 2013) and by Woods & Watson (1997). They both defined the bins only by wind direction. If the proportional relationship between wind speeds is applied, then the average wind speed in the simulated period at the target series inside each bin k_c is:

$$\bar{v}_c^d(k_c) = \frac{\sum_{k_r=1}^{N_{kr}}[p^d(k_r, k_c) * \bar{v}_c^d(k_r, k_c)]}{p^d(k_c)} \tag{7}$$

$$= \frac{\sum_{k_r=1}^{N_{kr}}\left[p^t(k_r, k_c)\dfrac{p^d(k_r)}{p^t(k_r)} * \bar{v}_c^t(k_r, k_c)\dfrac{\bar{v}_r^d(k_r)}{\bar{v}_r^t(k_r)}\right]}{p^d(k_c)}$$

where $\bar{v}_c^t(k_r, k_c)$ is the average wind speed at the target site in the training period for the cases, when the data fall jointly into the bins k_r and k_c at the reference and target series. Also *Moulded site method* described by King & Hurley (2004) uses an analogous principle, although it is not easily obvious.

Alternatively, a conditional probability density functions can be applied instead of separating data into bins. This method allows a calculation of the continuous wind speed distribution (Perea et al., 2011, Carta & Velázquez, 2011).

Besides the described types of MCP method, many further alternative approaches have been described in literature. Frequently mentioned is the employment of artificial neural networks (e.g. Bilgili et al., 2007, Albrecht & Klesitz, 2007). Two-dimensional linear regression was proposed by Achberger et al. (2002) or Nielsen et al. (2001, in Carta et al., 2011), but its performance according to the comparison done by Rogers et al. (2005) is poor. Also other alternative approaches do not show obvious advantages against the above mentioned methods.

3.2 Author's matrix MCP methods

The proposed methods, which are simply labeled as *Method 1* and *Method 2*, aim to remove some essential limitations of both above-described types of matrix methods. The calculation procedure is similar for both methods. At first all data are separated into bins k by the reference data and all time records are assigned to appropriate bins. Then every time record T^d of the simulated period is linked with a individual time record T^t of the training period belonging to the same bin. As a result, a synthetic wind data series is obtained, which preserves the joint relationship between the wind speed and wind direction.

Method 1 simply takes the ratio of wind speeds and the difference of wind directions (wind veer) from the time record T^t are applies it on the reference data of the time record T^d of the same bin k:

$$D_c(T^d) = D_r(T^d) + [D_c(T^t) - D_r(T^t)]$$

$$v_c(T^d) = v_r(T^d) * \frac{v_c(T^t)}{v_r(T^t)} \tag{8}$$

$$T^d \in k, T^t \in k$$

Finally, a correction is applied to the simulated wind speeds, so that the ratio $\frac{\bar{v}_c^t(k)}{\bar{v}_r^t(k)}$ of the average wind speed for individual bins is preserved.

Method 2 is principally based on the analysis of joint probability between bins defined by reference (k_c) and by target (k_r) series as described by (6) and (7). However, it includes an improvement and a generalization of this methodology. In the existing methods (Salmon & Walmsley, 1999, García-Rojo, 2004, Harstveit (2004, in Carta et al., 2013), Woods & Watson (1997)) the bins k_c and k_r have been defined and treated equally. But this is not necessary as bins k_r and k_c play different roles. Bins k_r have the same effect as the data classification (binning) in other above mentioned methods, while bins k_c just define the resolution of result. The only exception is when the method requires a minimal amount of training data in "combined" bins (k_r, k_c) as in the method of Woods & Watson (1997). Otherwise the dimension of bins k_c can be arbitrary and even infinitely small. In such case every time record of training data can be assigned to one unique bin k_c and the probabilities $p^d(k_c)$ inside one bin k_r are equal. Following (6), this effectively means, that a random time record T^t from training period, which belongs to the same bin k_r, can be assigned to the simulated record T^d. Similarly, the wind speed inside the bin k_c (i.e. the target wind speed $v_c(T^t)$ from the assigned time record) can be corrected according to the (7). As a result, a target series of wind data can be simulated as:

$$D_c(T^d) = D_c(T^t)$$
$$v_c(T^d) = v_c(T^t) * \frac{\bar{v}_r^d(k)}{\bar{v}_r^t(k)} \tag{9}$$
$$T^d \in k, T^t \in k$$

(k_r is simplified to k).

The appropriate definition of bins k (k_r) is fundamental for successful application of both methods. If the bins are too wide, then the methods are too rough and they lose their advantages against simpler methods. But high number of sparsely populated bins may cause increased random errors of individual bins. At the applied algorithm, the *basic classification* with large number of small bins is defined first. Then the small bins are merged, so that finally each applied *merged bin* contains at least pre-defined number of training data.

The applied algorithm for both methods includes an optimization, where the time records inside individual bins k are ranked according to the reference wind speed. Then the time records T^t with higher reference wind speed are assigned to records T^d with higher wind speed and vice versa (the overall number and distribution of used time records T^t inside the bin k is preserved, they are just re-ordered).

18

3.3 Comparison of MCP methods and reference data

A comparison was performed to verify the applicability of proposed methods and to compare various types of reference data sources. The wind data from manned weather stations were used as the target series. The same set of weather station data and the data from reanalyses were used as the reference series. The time period was limited to the years 2005-2008 to prevent the possible inhomogeneity and all data were adjusted to hourly data interval.

To enable multiple calculations for one pair of data series, one year of data was set up as a training set and the other three years were used for verification. In individual instances (runs) the training data consisted from 4 sections, each covering 3 consecutive moths. It was required that as a whole, the training data always covered all seasons. This way, set of 50 randomly chosen training periods was used in calculation.

The applied set of weather stations is shown at Table 2. All combinations of reference/target stations were initially calculated, including those, that would not be applied in practice because of large distance between them. The applied set of reanalysis data is shown in Table 3. The data from NCEP/NCAR (Kalnay et al., 1996), ERA Interim (Dee et al., 2011) and MERRA (Rienecker et al., 2011) reanalyses were used.

	alt.[m]	Doksany	Kopisty	B-Tuřany	O-Porub.	P-Libuš	Kuchař.	P-Ruzyně	Č.Buděj.	Cheb	Luká	K.Mysl.	Mileš.
Doksany	158		40	232	294	54	223	40	168	134	219	171	20
Kopisty	240	40		269	334	84	256	67	186	103	258	202	22
Brno-Tuřany	241	232	269		129	188	54	205	164	327	58	92	252
Ostrava-Poruba	242	294	334	129		267	184	282	285	415	89	211	313
Praha-Libuš	300	54	84	188	267		173	17	116	147	185	119	71
Kuchařovice	335	223	256	54	184	173		190	119	298	107	57	242
Praha-Ruzyně	364	40	67	205	282	17	190		128	133	200	135	56
České Budějovice	388	168	186	164	285	116	119	128		194	196	74	181
Cheb	483	134	103	327	415	147	298	133	194		331	242	122
Luká	511	219	258	58	89	185	107	200	196	331		123	238
Kostelní Myslová	563	171	202	92	211	119	57	135	74	242	123		189
Milešovka	833	20	22	252	313	71	242	56	181	122	238	189	

Table 2 *The applied set of weather stations including the distance between them (in km). The distances over 100 km are written by red, similarly as at Table 4.*

To evaluate the model results, six metrics were used: difference of average wind speeds (*h1*), difference of average power densities (*h2*), Kolmogorov-Smirnov integral (KSI) (Zhang et al., 2013, Boyo & Adeyemi, 2012) of differences between frequency distributions, corrected for the difference of average wind speed (*h3*), the average sector-wise difference of wind direction frequencies (*h4*), KSI of differences between wind direction distributions (*h5*) and the root-mean-square error (RMSE) of individual simulated records of wind speed (*h6*). Metrics *h1*, *h2* and *h6* were calculated as a percentage of real average wind speed, metric *h2* as a percentage of real average power density. Out of 50 runs calculated for each test, RMSE (or RMS – root mean square value), absolute maximal error (absmax) and bias were determined.

shortcut	reanalysis	temporal resolution	spatial resolution	pressure/height level	data type
nc_925g	NCEP/NCAR	6h	2.5 × 2.5°	925 hPa	geostrophic wind
nc_925w	NCEP/NCAR	6h	2.5 × 2.5°	925 hPa	model wind
nc_850g	NCEP/NCAR	6h	2.5 × 2.5°	850 hPa	geostrophic wind
nc_850w	NCEP/NCAR	6h	2.5 × 2.5°	850 hPa	model wind
era_1000g	ERA Interim	6h	0.75 × 0.75°	1000 hPa	geostrophic wind
era_1000w	ERA Interim	6h	0.75 × 0.75°	1000 hPa	model wind
era_925g	ERA Interim	6h	0.75 × 0.75°	925 hPa	geostrophic wind
era_925w	ERA Interim	6h	0.75 × 0.75°	925 hPa	model wind
era_850g	ERA Interim	6h	0.75 × 0.75°	850 hPa	geostrophic wind
era_850w	ERA Interim	6h	0.75 × 0.75°	850 hPa	model wind
me_2m	MERRA	1h	0.33 × 0.5°	2 m above ground	model wind
me_10m	MERRA	1h	0.33 × 0.5°	10 m above ground	model wind
me_50m	MERRA	1h	0.33 × 0.5°	50 m above ground	model wind
me1_850g	MERRA	1h	0.33 × 0.5°	850 hPa	geostrophic wind
me1_850w	MERRA	1h	0.33 × 0.5°	850 hPa	model wind

Table 3 *The overview of applied reanalysis data sets..*

As a basic setting, the bins were defined by 36 wind directions and by several unequal intervals of wind speed. The merged bins were required to contain at least 6 records of the training period. An example of simulation of Method 1 under these conditions is shown at Figure 10.
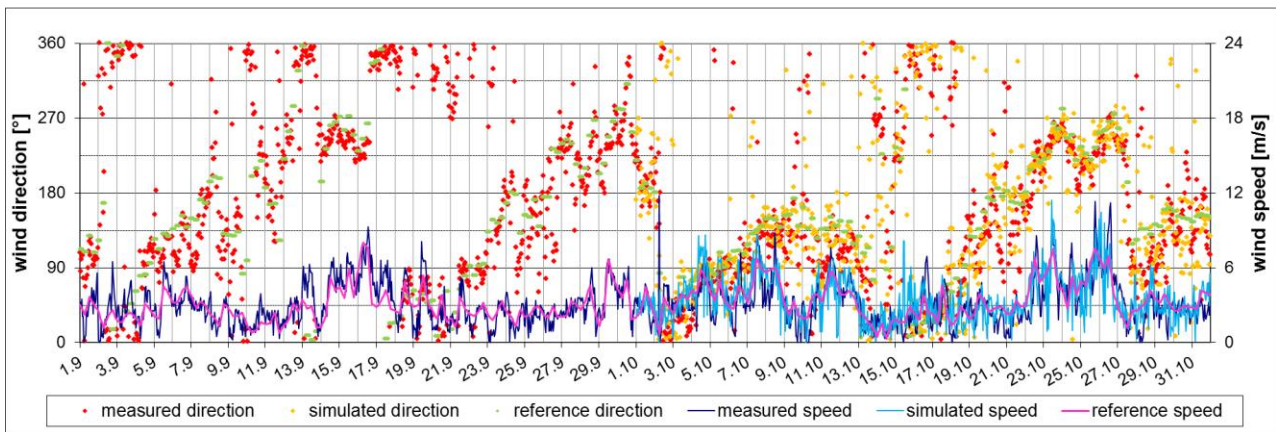
Figure 10 *The example of MCP Method 1 simulation and verification. The target series is Praha-Ruzyně, the reference series is era_1000w.*

Table 4 shows the RMSE of metric *h1* (average wind speed) for all calculated combinations of the reference and target series. It can be concluded, that if the reference and/or target wind data are measured at sites in lowlands and basins (Doksany, Kopisty, Brno-Tuřany, Ostrava-Poruba, Cheb), then large errors can be expected. This may be caused by the fact, that the wind conditions in such sites are frequently isolated from the

large-scale flow patterns due to inversions or local circulation, so that the interrelationship of local wind conditions to the other wind data series is weak. The strong orographic deformation of wind flow (Ostrava-Poruba, Kopisty) is an additional negative factor for reference series (but not for target series).

reference series	target series												avg.
	Doksany	Kopisty	B-Tuřan	O-Porub	P-Libuš	Kuchař.	P-Ruzyn	Č.Buděj.	Cheb	Luká	K.Mysl.	Mileš.	
Doksany		7.68%	8.97%	5.16%	3.98%	5.27%	4.07%	5.83%	7.97%	5.64%	4.58%	4.11%	**5.75%**
Kopisty	9.72%		11.29%	6.17%	7.33%	7.87%	7.38%	8.10%	8.64%	9.06%	8.81%	7.20%	**8.32%**
B-Tuřany	8.51%	6.61%		5.16%	3.73%	2.97%	4.29%	4.43%	4.07%	3.88%	5.71%	3.95%	**4.85%**
O-Poruba	10.73%	6.41%	7.75%		6.06%	6.40%	6.87%	7.06%	6.69%	7.08%	8.46%	6.26%	**7.25%**
P-Libuš	5.79%	5.52%	6.12%	3.97%		2.99%	1.27%	3.33%	4.86%	3.90%	4.19%	2.45%	**4.04%**
Kuchařovice	6.79%	5.65%	5.32%	4.34%	2.55%		3.14%	3.79%	4.77%	3.51%	4.22%	3.33%	**4.31%**
P-Ruzyně	5.59%	5.36%	6.23%	3.70%	1.11%	2.97%		3.16%	4.90%	3.82%	3.97%	2.16%	**3.91%**
Č.Buděj.	7.33%	4.91%	5.80%	4.86%	2.27%	3.04%	2.63%		4.35%	3.97%	4.24%	2.66%	**4.19%**
Cheb	9.64%	5.99%	5.57%	5.66%	4.35%	4.39%	4.92%	4.41%		5.05%	6.55%	4.56%	**5.55%**
Luká	6.98%	5.74%	5.45%	4.74%	2.51%	2.94%	3.01%	3.81%	4.97%		4.59%	2.77%	**4.32%**
K.Myslová	5.61%	6.44%	7.36%	4.66%	2.65%	3.28%	2.94%	4.03%	6.95%	3.83%		2.34%	**4.55%**
Milešovka	7.23%	5.61%	6.83%	3.61%	2.36%	3.08%	2.18%	4.03%	5.39%	4.52%	4.20%		**4.46%**
nc_925g	6.95%	5.01%	6.36%	4.62%	1.73%	1.62%	1.77%	3.17%	4.75%	3.11%	3.71%	1.38%	**3.68%**
nc_925w	6.41%	5.10%	6.86%	4.24%	1.83%	2.18%	1.74%	3.17%	5.59%	3.70%	3.53%	1.48%	**3.82%**
nc_850g	6.64%	5.36%	6.34%	5.05%	1.86%	2.02%	2.05%	3.05%	4.80%	3.09%	4.27%	1.89%	**3.87%**
nc_850w	6.45%	5.01%	6.86%	4.96%	2.07%	2.01%	2.12%	2.82%	5.75%	3.22%	3.76%	1.52%	**3.88%**
era_1000g	6.64%	5.83%	5.41%	3.31%	1.56%	1.74%	1.80%	4.13%	5.19%	3.47%	4.12%	1.91%	**3.76%**
era_1000w	5.92%	5.59%	4.96%	3.23%	1.24%	1.45%	1.11%	3.41%	5.21%	2.49%	3.97%	1.60%	**3.35%**
era_925g	6.77%	5.03%	5.68%	3.56%	1.40%	1.92%	1.51%	3.76%	5.23%	3.12%	4.05%	1.18%	**3.60%**
era_925w	6.52%	5.23%	5.87%	3.44%	1.73%	1.97%	1.69%	3.28%	4.89%	2.89%	3.86%	1.32%	**3.56%**
era_850g	6.50%	4.84%	6.28%	3.83%	1.79%	1.86%	1.86%	2.90%	5.09%	3.46%	4.23%	1.43%	**3.67%**
era_850w	6.59%	4.57%	6.79%	4.05%	1.92%	2.02%	1.94%	3.41%	5.14%	3.46%	3.87%	1.02%	**3.73%**
me_2m	6.46%	5.64%	5.67%	3.61%	1.29%	1.71%	1.46%	3.53%	5.02%	2.63%	3.78%	1.43%	**3.52%**
me_10m	6.51%	5.50%	5.64%	3.54%	1.26%	1.65%	1.37%	2.98%	5.13%	2.55%	3.78%	1.35%	**3.44%**
me_50m	6.44%	5.51%	5.64%	3.54%	1.25%	1.63%	1.33%	2.81%	5.13%	2.45%	3.67%	1.30%	**3.39%**
me1_850g	6.96%	5.24%	6.42%	4.05%	2.08%	2.34%	2.04%	3.14%	5.10%	3.95%	3.92%	1.39%	**3.89%**
me1_850w	6.68%	4.94%	6.54%	4.19%	2.06%	2.00%	2.06%	3.04%	5.68%	3.02%	3.63%	1.24%	**3.76%**
avg.	**7.03%**	**5.58%**	**6.46%**	**4.28%**	**2.48%**	**2.85%**	**2.66%**	**3.90%**	**5.42%**	**3.91%**	**4.56%**	**2.48%**	**4.33%**
Null method	11.20%	7.17%	7.58%	5.78%	5.45%	5.22%	6.91%	6.48%	6.59%	6.81%	6.45%	5.41%	**6.76%**

Table 4: *The RMSE of metrics h1 (difference between the average wind speeds) for all tested combinations of reference and target series. The Method 1 in standard settings was applied. The highest and lowest 3 values for each target series are highlighted, the results from pairs of weather stations in the distance of over 100 km are written red.*

For open sites, the 1000 hPa wind from ERA reanalysis and the surface wind from MERRA reanalysis are generally the best reference series. The exception, when the measured data as reference series are better than reanalyses, is the case when they are measured at near-by topographically similar sites (Praha-Ruzyně × Praha-Libuš).

The results for metrics *h2*, *h3* and *h6* are basically similar. For the wind rose metrics *h4* and *h5* also the shape of target site wind rose plays role (the omnidirectional target wind roses tend to show better results than the wind roses with one or two strongly prevailing wind directions for both metrics).

Figure 11 compares the "improvement rate" of RMSE of *h1* metrics against the Pearson correlation coefficient between the individual records of reference and target series. The *improvement rate* is a ratio between the RMSE of applied Method 1 and the *Null method*, which takes the training data of target series as a simulation result. At the "improper" reference series from low-lying sites (Doksany, Kopisty, Brno-Tuřany, Ostrava-Poruba a Cheb), the result is chaotic and improvement is generally poor. In the other cases, the error is reduced as much as to 20 % for the best correlated series (r > 0.75). For the series with correlation of 0.5-0.6, which is marked as "very poor correlation" by EMD International (2008), the method still improves the results to 40 – 80 % of RMSE of Null method.
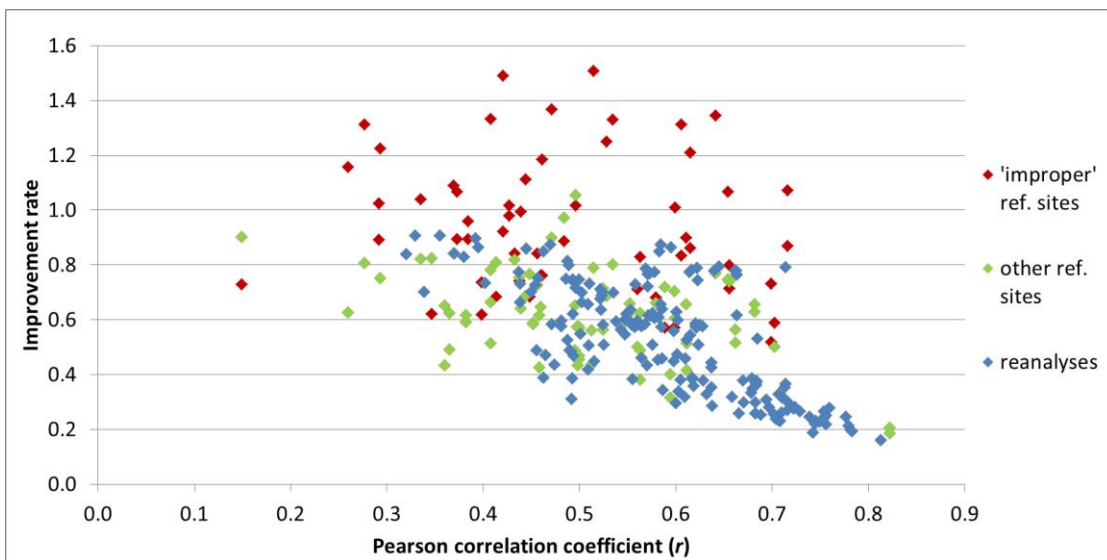
Figure 11 *The "improvement rate" of Method 1 vs. the correlation between reference and target data. The results are differentiated by the reference data source. See text for more explanation.*

The comparison between the author's methods and basic MCP methods (Table 5) shows that both Method 1 and Method 2 perform well. The accuracy of simulation of the average wind speed (*h1*) is similar to the Linear regression (*linReg*) method (4) and better than for the Method of ratios (*ratios*) (1) and the Variance ratio (*varRat*) method (5). The results of *h2* and *h3* metrics for the Linear regression method and the Method of ratios without simulation of residual are not relevant, because these methods are not designed to the calculation of the wind speed frequency distribution. Among the other methods, the Method 1 a Method 2 are much better then the Variance ratio method. On the other hand the Method 1 and Method 2 are less successful then the simpler methods in simulation of individual values of wind speed due to their wind variability simulation.

The result also shows that the classification of wind data by wind direction clearly improves results of all methods. However, it cannot be clearly concluded that the basic classification to 36 directional sectors improves the result against classification to 12 sectors, because the result depends on other factors (used data, rate of binning by other factors, merging algorithm, minimum number of training data inside bin etc.).

method	DD	h1 (% of wind speed)			h2 (% of power density)			h3 (% sp.)	h6 (% sp.)
		RMSE	absmax	bias	RMSE	absmax	bias	RMS	RMS
ratios	1	4.19%	9.13%	0.23%	31.6%	48.6%	-17.21%	13.54%	57.4%
ratios	12	4.03%	8.74%	0.61%	26.1%	43.3%	-11.19%	10.88%	53.8%
ratios	36	4.08%	8.90%	0.79%	25.8%	43.8%	-9.79%	10.65%	53.8%
linReg	1	3.68%	8.10%	-0.35%	42.7%	58.9%	-41.97%	22.94%	53.8%
linReg	12	3.33%	7.32%	-0.16%	34.6%	49.0%	-33.90%	18.32%	49.9%
linReg	36	3.28%	7.31%	-0.26%	32.9%	47.5%	-32.08%	17.45%	49.9%
varRat	1	4.74%	10.37%	1.26%	12.3%	27.8%	0.15%	4.80%	60.4%
varRat	12	4.47%	9.73%	1.71%	12.0%	26.0%	3.46%	4.02%	56.8%
varRat	36	4.60%	9.87%	2.05%	14.2%	29.3%	6.94%	4.04%	57.1%
m1	1	3.58%	7.63%	-0.14%	9.8%	22.1%	-0.93%	3.24%	74.8%
m1	12	3.36%	7.12%	0.14%	8.8%	19.3%	-0.03%	2.91%	69.0%
m1	36	3.32%	7.20%	0.17%	9.1%	19.5%	0.85%	2.91%	68.5%
m2	1	3.58%	7.63%	-0.15%	9.9%	22.0%	-1.23%	3.27%	74.9%
m2	12	3.37%	7.15%	0.14%	8.8%	19.5%	-0.87%	2.94%	69.0%
m2	36	3.32%	7.24%	0.17%	8.8%	20.5%	-0.86%	2.92%	68.5%
avg		**3.80%**	**8.23%**	**0.41%**	**19.2%**	**33.1%**	**-9.24%**	**8.32%**	**61.2%**
Null method		*6.30%*	*13.90%*	*-0.87%*	*20.9%*	*44.3%*	*-3.40%*	*5.08%*	*95.1%*

Table 5 *The average values of test results for different MCP methods.*

Figure 12 shows an example of the wind rose simulation. In this aspect, both Method 1 and Method 2 perform very well.
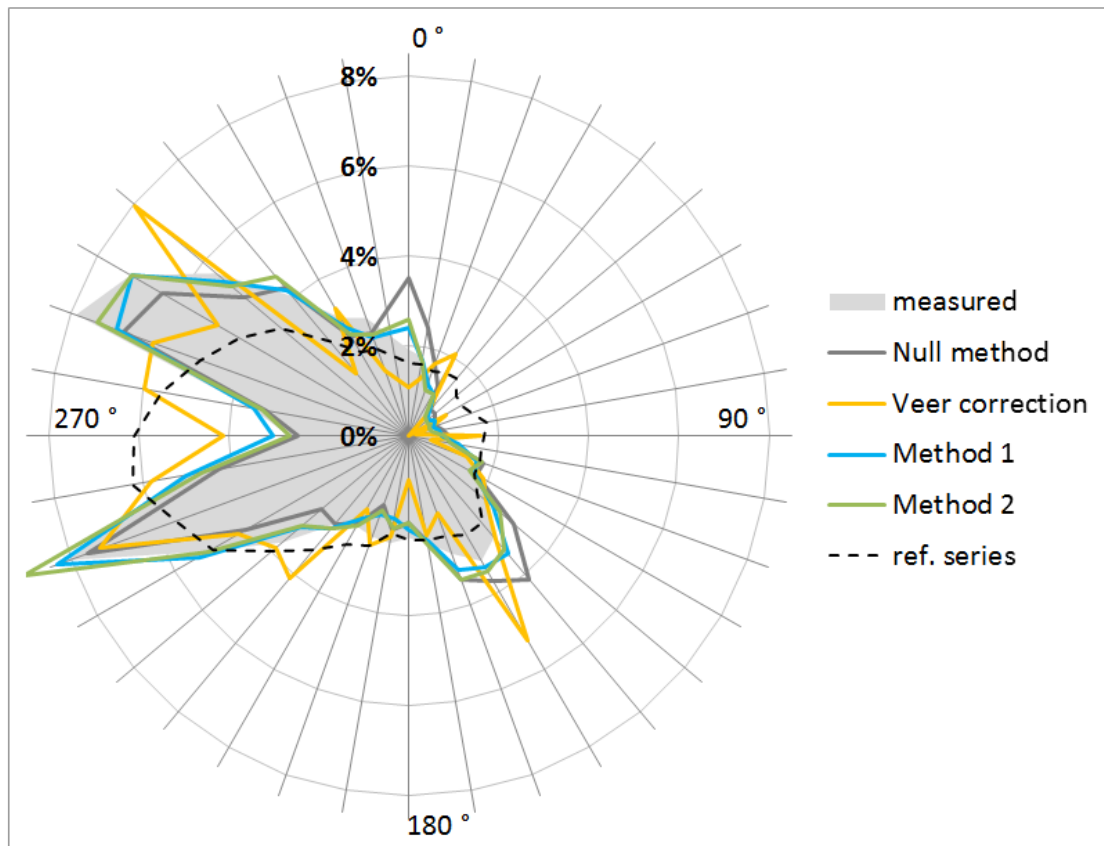
Figure 12 *The example of one individual run of wind rose simulation for the target series Milešovka (reference series me_10m).*

The comparison of various settings of the Method 1 and Method 2 was done as well. It was found, among others, that:

- it is difficult to say, whether an additional classification (binning) by daytime and season improves the result. Its effect depends on chosen pair of reference/target data series and on other settings of applied method. In general, an additional classification rather improves results if the other classifications are less detailed (i.e. number of wind direction sectors is lower) and if the minimum required number of training data in a merged bin is lower and vice versa,

- the chosen minimum number of 6 training records in a merged bin (for wind data of 1h time resolution) is close to optimal, but removing the limit (i.e. one training record in a bin is accepted) or increasing the limit to the minimum of 12 records gives similar results. Higher number of required records in a merged bin leads to higher errors, especially if the basic classification is more detailed,

- the optimization of assigning ranked data inside bins generally improves results,

- the correction for ratio of average wind speeds (inside bins) in Method 1 improves results slightly. Most notably it decreases positive bias of this method, that would otherwise appear,

- the effect of wind speed correction $\frac{\bar{v}_r^d(k)}{\bar{v}_r^t(k)}$ in Method 2 is substantial. It improves results of average wind speed, average power density and frequency distribution. This improvement effectively indicates the difference between Method 2 and methods of Salmon & Walmsley (1999) or García-Rojo (2004).

4. Wind climate of the Czech Republic

4.1 General properties of the wind climate

In agreement with Sobíšek (2000), the surface wind climate at any site (not only) in the Czech Republic can be understood as a result of three factors: geostrophic wind conditions, regional thermal and radiation effects and topographic effects. These factors manifest differently in different sites. In open elevated sites the wind conditions are mostly driven by the wind flow in free atmosphere, while in sites less exposed the local circulations and effects of local obstacles play important role.

Majority of the studies of the wind climate in the Czech Republic, that were found by the author of this thesis, focus predominantly to the descriptive analysis of wind measurements (e.g. Kolektiv autorů, 1958, Sobíšek, 2000, Tolasz et al., 2007 and many local studies). The general interpretation of measured wind patterns over the area of

former Czechoslovakia was performed in a study Petrovič et al. (1969), where the diurnal and seasonal periodicity of wind speed and wind direction were analyzed. The effort was also made by Stuchlíka & Křivánkové (1966) and Sobíšek (1969, 1982, 1992, 1995, 2000) to generalize the wind conditions spatially by definition of "wind climatic regions", based on the prevailing wind directions. However, the design of such areas depends on the choice of used wind measurements and it cannot capture the complex spatial variability of wind conditions.

Two specific wind phenomena in the Czech Republic were identified besides the general pattern of dominant wind flow from western directions. The well known feature is the episodic regional increase of wind speed from south to south-east directions, which occurs over wide belt from southeast Moravia across the country up to north Bohemia. It is related to the streaming of wind through the gap between Alps and Carpathians (Defant, 1923, Gregor, 1957). As the air stratification is stable, the low-level jet stream can develop in such situations (Brázdil & Štekl (1986)). Additionally, the foehn wind can occur at the lee sides of Carpathians in south and east Moravia (Gregor, 1953).

The second notable phenomena is the cold downslope "polák" wind from north to north-east, occurring over the lee sides of mountains Orlické hory, Jeseníky and in Moravská brána channel (ČMeS, 2014). It can be probably classified as weak bora wind. According to the findings of author of this thesis, this feature can be found also in middle and southeastern Moravia (Figure 13).
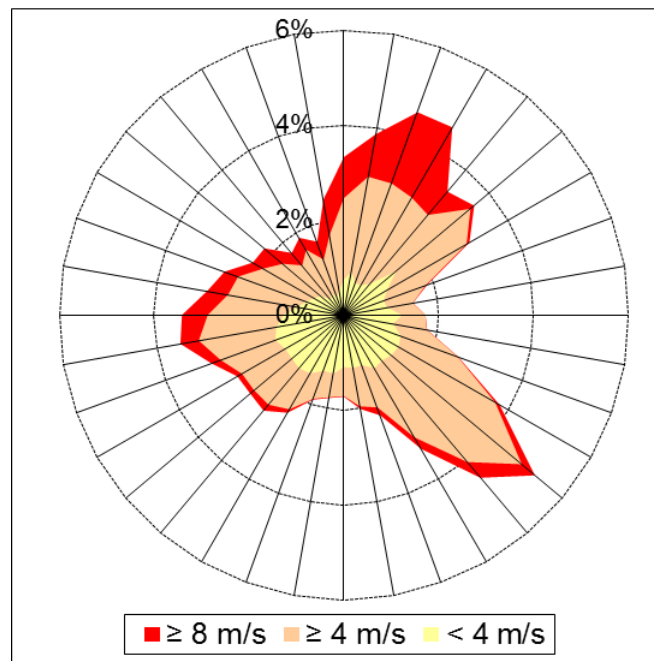
Figure 13 *The wind rose (1 year of measurement) for a site in mid-southeastern Moravia, at the southern slopes of mid-Moravian Carpathians. Three prevailing wind directions can be identified: i) the north-northeastern "polák" wind, intensified here by the its downslope movement, ii) the south-eastern wind typical for southeast Moravia, iii) western wind flow, which is relatively weak compared to the Bohemian regions.*

4.2 Wind map of the Czech Republic

(The wind map described here was created in cooperation between Jiří Hošek and author of this thesis, with technical help of our colleagues.)

The main purpose of the construction of the "Wind map" is to estimate the wind conditions over the Czech Republic for needs of possible wind energy utilization. Several "wind maps" have been therefore constructed in the past 20 years with various level of success (Hanslian et al., 2012). The actual wind map, described in this thesis, was calculated as a combination of models VAS/WAsP and PIAP:

The *VAS/WAsP model* (Hanslian et al., 2012) is a combination of VAS method and WAsP model. VAS (Sokol & Štekl, 1994) is a method for three-dimensional interpolation of meteorological variables. If applied to the wind data, this method reflects the general increase of wind speed with altitude, that can be observed in the Czech republic. WAsP model (Troen & Petersen, 1989) is the widely used wind resource assessment model, which enables detailed evaluation of effects of local terrain, roughness changes and obstacles on wind conditions. The combined VAS/WAsP model consists from three steps: At first the wind measurements are processed by WAsP to remove the local effects from measured data and obtain the "generalized wind conditions". Then the generalized data are interpolated by VAS. Finally, a detailed calculation over the whole area is performed again by WAsP in order to include the effects of local orography and roughness. This approach captures both large-scale and microscale effects on wind conditions. Its performance is, however, limited in microscale due to simplified physics of the model WAsP, so that the effects of steep or complex orographic features cannot be well captured. In larger scales the accuracy of VAS/WAsP is limited by lack of flow modelling, so that its performance depends on the number (and quality) of applied wind measurements.

The *PIAP model* (Svoboda et al., 2013) is non-hydrostatic and non-stationary boundary layer model for numerical simulation of flow over hilly landscape. The calculation consists of the numerical simulation of pre-defined scenarios and the statistical model, in which the scenarios are adjusted and weighted by wind conditions at reference site. Based on the single wind measurement the PIAP model can simulate wind conditions over extensive area, considering the effects of orography at various scales. However, it requires much more computing time than VAS/WAsP model and several limitations of the accuracy of its simulation exists.

To calculate the wind map, wind measurements from various sources were considered:

- the wind data from (both manned and unmanned) meteorological stations. These data are rather of good quality (especially data from manned stations) and usually available for long time period, but they often suffer form poor anemometer siting and inhomogeneties,

- the wind data from wind masts. They are usually only short-term (1 or 2 years), but well sited and mostly of good quality,

- the wind measurements at air quality (AIM) measurement network. The data quality varies, but some of the stations are well sited at areas with no other wind data available.

The wind data underwent thorough data and measurement site quality control and the most problematic data records were removed. The MCP Method 2 (see chapter 3.1 for details) was applied to extend all data to the period 1997-2006.

Finally, 71 wind measurements were applied in calculation of VAS/WAsP model. Calculation of PIAP model was only based on 5 wind measurements. The CORINE (Haines-Young et al., 2006) data were used for classification of surface roughness according to the study of Wieringa (2003). The digital terrain model DMÚ25 was used for orography description.

The results of calculation of VAS/WAsP model are shown at Figure 14 and 15, the result of PIAP calculation is shown in Figure 16. The final result (Figure 17) was simply calculated as weighted average of VAS/WAsP and PIAP results in the ratio 7 : 3. The calculation of PIAP was originally performed in a grid with resolution of 600 m, so it had to be resampled to the 100-meter resolution of VAS/WAsP model. The height above ground for wind map was set to 100 m, which is the typical height of wind turbines.

According to the final wind map, the highest average wind speed can be expected on the ridges of Krkonoše and Jeseníky mountains. However, the largest areas with average wind speeds above 6 m/s that are theoretically suitable for wind power utilization exist over the highland areas of Krušné hory, Českomoravská vrchovina, Nízký Jeseník and others.
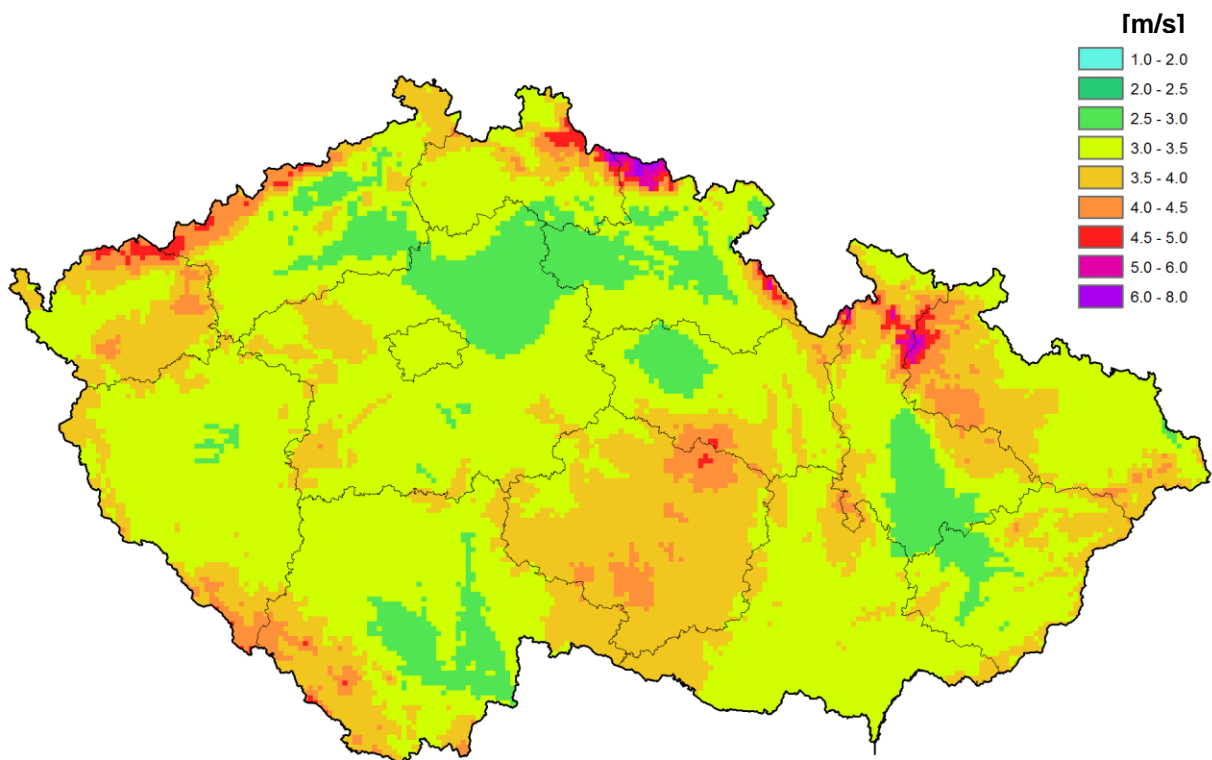
Figure 14 *Result of interpolation by the VAS method in the VAS/WAsP model for roughness length of 0.1 m and height 10 m. Author of the illustration: Jiří Hošek.*
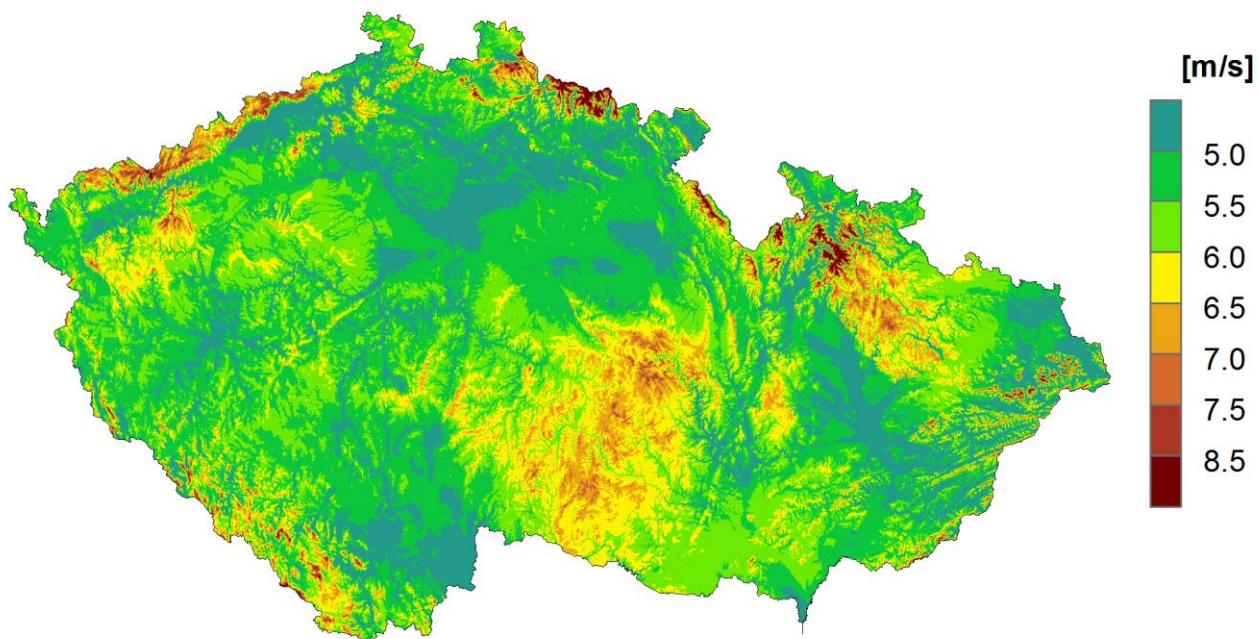
Figure 15 *VAS/WAsP model – average wind speed at the height of 100 m above ground. Author of the illustration: Jiří Hošek.*
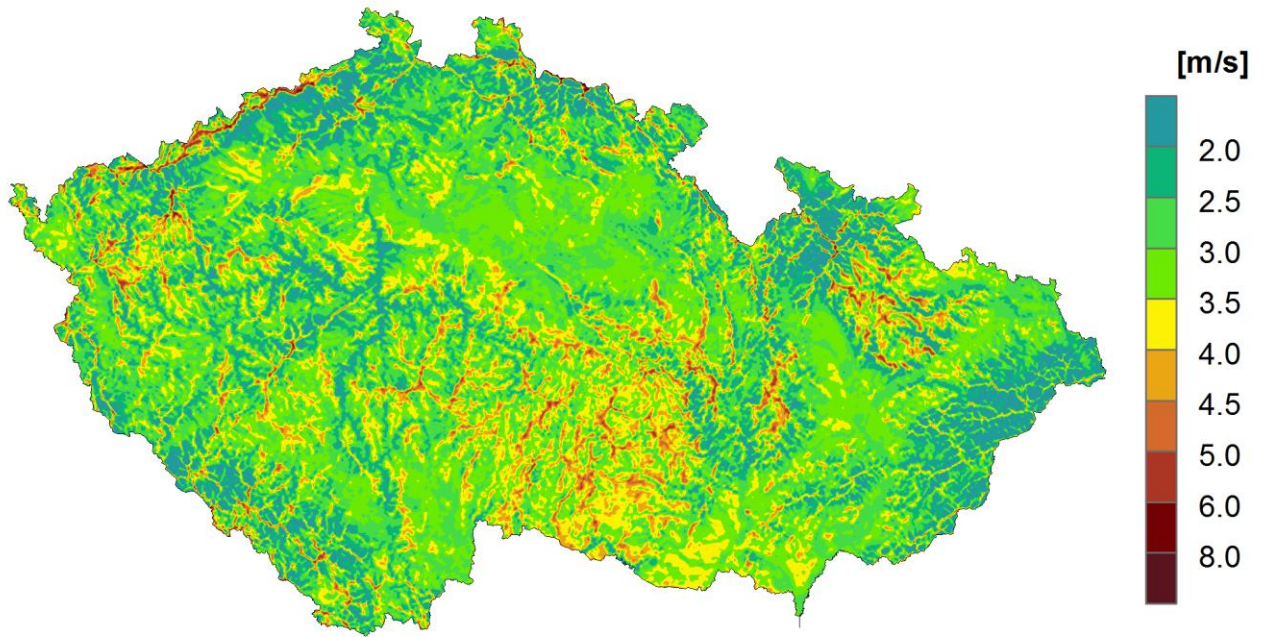
Figure 16 *PIAP model – average wind speed at the height of 10 m above ground. Author of the illustration: Jiří Hošek*
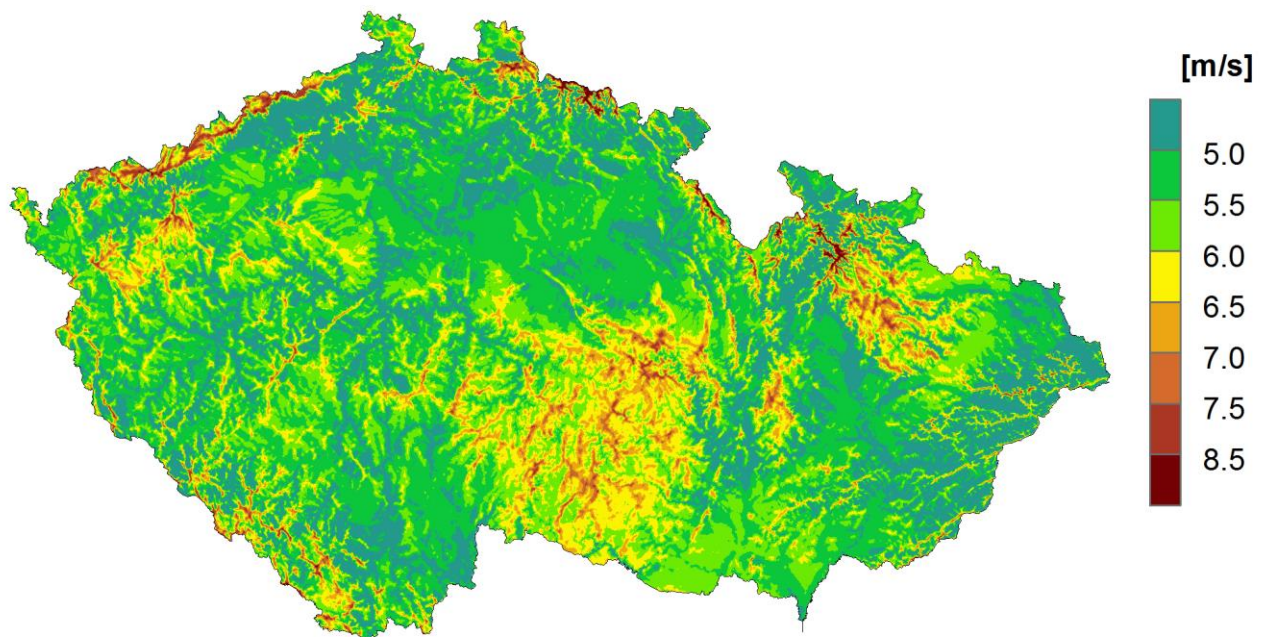
Figure 17 *Resulting wind map – average wind speed at the height of 100 m above ground. Author of the illustration: Jiří Hošek*

The accuracy of the wind map was verified by comparison with wind measurements that were not available at the time of its calculation. These wind data were measured on wind masts at the heights 35 - 90 m above ground and transformed to the height of 100 m using WAsP model. They were also extended to the period 1997-2006 by Method 2 (chapter 3.2). As a result, the errors of spatial extrapolation of wind data are fully considered, while the errors of wind profile simulation by WAsP and long-term correction are considered only partially.

The result (Table 6) shows, that the RMSE of average wind speed calculation was 0.4 m/s and the simulated wind speeds were positively biased by almost 0.3 m/s. The most probable main source of the overestimation of simulated wind speed is the position of wind speed measurement at manned weather stations above roof (see chapter 2.2). Even though some correction of wind speed at these measurements was applied, it was probably not sufficient to fully cover the real wind speed-up.

ID	altitude	z_0	RIX	altitude differences	difference against measurement [m/s]		
	[m]	[m]	[%]	[m]	VAS/WAsP	PIAP	wind map
A	200	0.12	0	-10/100	0,19	-0,27	0,05
B	300	0.08	0	-20/50	0,20	0,37	0,25
C	300	0.10	0.2	-100/50	0,12	-0,19	0,03
D	300	0.09	0	-70/100	0,54	0,83	0,63
E	400	0.12	0.9	-50/50	-0,38	-0,60	-0,44
F	400	0.20	1	-130/130	0,64	-0,18	0,39
G	400	0.24	5.7	-100/50	0,71	0,54	0,66
H	400	0.19	1.4	-120/200	0,10	0,40	0,19
I	500	0.27	0.6	-150/50	0,02	0,63	0,20
J	500	0.28	0.6	-100/50	0,03	0,64	0,21
K	600	0.19	1.8	-200/10	-0,07	1,20	0,31
L	600	0.22	3.9	-150/200	-0,23	1,12	0,18
O	600	0.22	2.1	-200/0	0,53	1,04	0,68
P	700	0.18	2.1	-200/100	0,83	0,09	0,61
Q	700	0.17	0.2	-100/30	0,26	0,97	0,47
R	700	0.35	0.8	-200/130	0,28	-1,01	-0,11
root mean square error (RMSE)					**0.41**	**0.72**	**0.40**
bias					**0.24**	**0.35**	**0.27**

Table 6 *Comparison of the average wind speed by VAS/WAsP and PIAP model and by resulting wind map with the results derived from the independent wind mas measurements.*

References

Anderson, M. (2004). *A review of MCP techniques.* RES Report 01327R00022.

Achberger, C., Ekström, M., & Bärring, L. (2002). Estimation of local near-surface wind conditions–a comparison of WASP and regression based techniques. *Meteorological Applications*, **9**(2), 211-221.

Bilgili, M., Sahin, B., & Yasar, A. (2007). Application of artificial neural networks for the wind speed prediction of target station using reference stations data. *Renewable Energy*, **32**(14), 2350-2360.

Boyo, A. O., & Adeyemi, K. A. (2012). Analysis of Solar Radiation data From Satellite and Nigeria Meteorolocical Station. *International Journal of Renewable Energy Research*, **1**(4), 314-322.

Brázdil, R., & Štekl, J. (1986). *Cirkulační poměry a atmosférické srážky na území ČSSR.* Univerzita J. E. Purkyně, Brno.

Brower, M. C., et al. (2012). *Wind resource assessment: a practical guide to developing a wind project.* M. Brower (Ed.). John Wiley & Sons.

Brunskill, A. W., & Lubitz, W. D. (2012). A neural network shelter model for small wind turbine siting near single obstacles. *Wind & Structures*, **15**(1), 43-64.

Carta, J. A., & Velázquez, S. (2011). A new probabilistic method to estimate the long-term wind speed characteristics at a potential wind energy conversion site. *Energy*, **36**(5), 2671-2685.

Carta, J. A., Velázquez, S., & Cabrera, P. (2013). A review of measure-correlate-predict (MCP) methods used to estimate long-term wind characteristics at a target site. *Renewable and Sustainable Energy Reviews*, **27**, 362–400.

Clive, P. J. (2008). Non-linearity in MCP with Weibull distributed wind speeds. *Wind Engineering*, **32**(3), 319-323.

ČMeS (2014). *Meteorologický slovník terminologický a výkladový.* Pracovní elektronická verze. Cit. 15.2.2014.

Dee, D. P., Uppala, S. M., Simmons, A. J., Berrisford, P., Poli, P., Kobayashi, S., ... & Vitart, F. (2011). The ERA-Interim reanalysis: Configuration and performance of the data assimilation system. *Quarterly Journal of the Royal Meteorological Society*, **137**(656), 553-597.

Defant, A. (1924). *Die Windverhältnisse in Gebiete der ehemaligen Österr.-ungar. Monarchie*.

Dellwik, E., Landberg, L., & Jensen, N. O. (2004). *WAsP in the forest*. In: *Proceedings of the European wind energy conference*.

EMD International A/S (2008). *WindPRO 2.6 User Guide*. Aalborg, Denmark. Dostupné z: http://www.emd.dk/download/UK-WindPRO2.6-manual.pdf.

Enveco GmBH. *BDB Index – general information*. Dostupné z: http://enveco.de/enveco.php?lang=en&content=0301. Staženo 15.5.2014.

Farrugia, R. N., & Sant, T. (2013). Modelling wind speeds for cup anemometers mounted on opposite sides of a lattice tower: A case study. *Journal of Wind Engineering and Industrial Aerodynamics*, **115**, 173-183.

Foken, T. (2008). *Micrometeorology*. Springer.

García-Rojo, R. (2004). Algorithm for the estimation of the long-term wind climate at a meteorological mast using a joint probabilistic approach. *Wind Engineering*, **28**(2), 213-223.

Gregor, A. (1953). Příspěvek k charakteristice "místního" počasí na jižní Moravě. *Meteorologické Zprávy*, **6**, 53-57.

Gregor, Z. (1957). Orografické deformace jihovýchodního proudění ve střední Evropě. *Meteorologické Zprávy*, **10**, 3-6.

Haines-Young, R., Weber, J. L., et al. (2006). *Land accounts for Europe 1990–2000: Towards integrated land and ecosystem accounting*. EEA, Copenhagen, Denmark.

Hanslian, D., Chládová, Z., Pop, L., & Hošek, J. (2012). Modely pro konstrukci větrných map v ČR. *Meteorologické zprávy*, **65**(2), 36-44.

Harman, I. N., & Finnigan, J. J. (2007). A simple unified theory for flow in the canopy and roughness sublayer. *Boundary-layer meteorology*, **123**(2), 339-363.

Harstveit, K. (2004). Estimating long-term wind distributions from short-term data set using a reference station. In: *Proceedings of the European wind energy conference*.

IEA (1999). Recommended practices for wind turbine testing and evaluation. Wind speed measurement and use of cup anemometry.

Kalnay, E., Kanamitsu, M., Kistler, R., Collins, W., Deaven, D., Gandin, L., ... & Joseph, D. (1996). The NCEP/NCAR 40-year reanalysis

King, C., & Hurley, B. (2004). The Moulded Site Data (MSD) wind correlation method; description and assessment. *Wind Engineering*, **28**(6), 649-666.

King, C., & Hurley, B. (2005). The SpeedSort, DynaSort and Scatter wind correlation methods. *Wind Engineering*, **29**(3), 217-242.

Kolektiv autorů (1958). *Atlas podnebí Československé republiky*. Ústřední správa geodesie a kartografie, Praha.

Landberg, L. (2000). The mast on the house. *Wind Energy*, **3**(3), 113-119.

Lindelöw, P. J. P., Pedersen, F. T., Gottschall, J., Vesth, A., Wagner, R., Paulsen, S. U., & Courtney, M. (2010). *Flow distortion on boom mounted cup anemometers*. Danmarks Tekniske Universitet, Risø Nationallaboratoriet for Bæredygtig Energi.

MEASNET (2008). *Evaluation of site-specific wind conditions*. Version 1. Dostupné z: http://www.measnet.com/wp-content/uploads/2012/04/Measnet_SiteAssessment_V1-0.pdf

Mortimer, A. A. (1994). A new correlation/prediction method for potential wind farm sites. In *Proceeding of the 16th BWEA wind energy conference*.

Nielsen, M., Landberg, L., Mortensen, N. G., Barthelmie, R. J., & Joensen, A. (2001). Application of the measure-correlate-predict approach for wind resources assessment. In: *Proceedings of the European wind energy conference*, 773–776.

Oke, T. R. (2006). *Initial guidance to obtain representative meteorological observations at urban sites*. WMO, Instruments and observing methods report No. 81.

Orlando, S., Bale, A., & Johnson, D. A. (2011). Experimental study of the effect of tower shadow on anemometer readings. *Journal of Wind Engineering and Industrial Aerodynamics*, **99**(1), 1-6.

Perera, M. D. A. E. S. (1981). Shelter behind two-dimensional solid and porous fences. *Journal of Wind Engineering and Industrial Aerodynamics*, **8**(1), 93-104.

Perea, A. R., Amezcua, J., & Probst, O. (2011). Validation of three new measure-correlate-predict models for the long-term prospection of the wind resource. *Journal of Renewable and Sustainable Energy*, **3**(2).

Perrin, D., McMahon, N., Crane, M., Ruskin, H. J., Crane, L., & Hurley, B. (2007). The effect of a meteorological tower on its top-mounted anemometer. *Applied Energy*, **84**(4), 413-424.

Petrovič, Š., et al. (1969). *Podnebí ČSSR. Souborná studie*. Hydrometeorologický ústav, Praha.

Raupach, M. R. (1994). Simplified expressions for vegetation roughness length and zero-plane displacement as functions of canopy height and area index. Boundary-Layer Meteorology, 71(1-2), 211-216.

Riedel, V., Strack, M., & Waldl, H. P. (2001). Robust approximation of functional relationships between meteorological sata: alternative measure-correlate-predict algorithms. In *Proceedings of the European Wind Energy Conference*, 806-809.

Rienecker, M. M., Suarez, M. J., Gelaro, R., Todling, R., Bacmeister, J., Liu, E., ... & Molod, A. (2011). MERRA: NASA"s Modern-Era Retrospective Analysis for Research and Applications. *Journal of Climate*, **24**(14).

Rogers, A. L., Rogers, J. W., & Manwell, J. F. (2005). Comparison of the performance of four measure–correlate–predict algorithms. *Journal of Wind Engineering and Industrial Aerodynamics*, **93**(3), 243-264.

Salmon, J. R., & Walmsley, J. L. (1999). A two-site correlation model for wind speed, direction and energy estimates. *Journal of Wind Engineering and Industrial Aerodynamics*, **79**(3), 233-268.

Sobíšek, B. (1969). Reprezentativnost větroměrných údajů meteorologických stanic v České socialistické republice. In: *Sborník prací HMÚ*, **14**, HMÚ, Praha, 145-182.

Sobíšek, B. (1982). Metodika kvantitativního hodnocení reprezentativnosti větroměrných údajů získaných ve staniční síti. *Meteorologické Zprávy*, **35**, 103-107.

Sobíšek, B. (1992). Kontrola kvality větroměrných dat ve staniční síti v České republice v roce 1989. *Národní klimatický program*, **2**, Praha.

Sobíšek, B. (1995). Reprezentativnost větroměrných dat meteorologických stanic v období 1961-1990. *Meteorologické Zprávy*, **48**, 45-49.

Sobíšek, B. (2000). Rychlost a směr větru na území České republiky v období 1961-1990. *Národní klimatický program*, **29**, Praha, 86 s.

Sokol, Z. & Štekl, J. (1994). 3-D mesoscale analysis of selected elements from SYNOP and SYRED reports. *Meteorologische Zeitschrift*, **3**, 242–246.

Svoboda, J., Chladova, Z., Pop, L., & Hosek, J. (2013). Statistical-dynamical downscaling of wind roses over the Czech Republic. *Theoretical and Applied Climatology*, **112**(3-4), 713-722.

Stickland, M., Scanlon, T., Fabre, S., Oldroyd, A., & Mikkelsen, T. (2012, April). Measurement and simulation of the flow field around a triangular lattice meteorological mast. In *European Wind Energy Conference*.

Stuchlík, F., & Křivánková, H. (1966). Vymezení oblastí s převládajícími směry větru a rychlostí větru v západní polovině ČSSR, *Meteorologické Zprávy*, **19**, 43-48.

Tolasz, R., Brázdil, R., Bulíř, O., Dobrovolný, P., Dubrovský, M., Hájková, L., ... & Žalud, Z. (2007). *Altas podnebí Česka*. Český hydrometeorologický ústav, Universita Palackého.

Troen, I. E. L. P., & Petersen, E. L. (1989). *European wind atlas*. Risø National Laboratory.

Verhoef, A., McNaughton, K. G., & Jacobs, A. F. G. (1997). A parameterization of momentum roughness length and displacement height for a wide range of canopy densities. *Hydrology and Earth System Sciences Discussions*, **1**(1), 81-91.

Wieringa, J. (1993). Representative roughness parameters for homogeneous terrain. *Boundary-Layer Meteorology*, **63**(4), 323-363.

WMO (2008). *Guide to Meteorological Instruments and Methods of Observation.*

Woods, J. C., & Watson, S. J. (1997). A new matrix method of predicting long-term wind roses with MCP. *Journal of Wind Engineering and Industrial Aerodynamics*, **66**(2), 85-94.

Zhang, J., Hodge, B. M., Florita, A., Lu, S., Hamann H. F., & Banunarayanan V. (2013). Metrics for evaluating the accuracy of solar power forecasting. To be presented at *3rd International Workshop on Integration of Solar Power into Power Systems*, London, England.

List of publications

(reviewed)

Kolektiv autorů (2010): *Větrná energie v České republice: hodnocení prostorových vztahů, environmentálních aspektů a socioekonomických souvislostí*. Ústav Geoniky AV ČR, Brno, 208 s. ISBN 978 -80 -86407 -84 -5; ; Štekl, J., **Hanslian, D.**, Hošek, J., Pop, L., & Svoboda, J.: kapitoly 1 a 2, 16-54.

Hanslian, D. (2011). Technický potenciál větrné energie v České republice. *Energetika*, **61**(8-9), 467-471.

Kolektiv autorů (2012): *Obnovitelné zdroje energie.* Profi Press, Praha, 208 s. ISBN 978-80-86726-48-9; **Hanslian, D.**: kapitola Větrné elektrárny, 116-139.

Hanslian D. (2012): Větrné podmínky pro malé větrné elektrárny. *TZB-info*, 12.3.2012. http://oze.tzb-info.cz/vetrna-energie/8358-vetrne-podminky-pro-male-vetrne-elektrarny

Hanslian, D., Chládová, Z., Pop, L., & Hošek, J. (2012). Modely pro konstrukci větrných map v ČR. *Meteorologické zprávy*, **65**(2), 36-44.

Hanslian, D., Hošek, J., Chládová, Z., & Pop, L. (2013). Větrné podmínky v České republice ve výšce 10 m nad povrchem I. *TZB-info*, 15.4.2013. http://oze.tzb-info.cz/vetrna-energie/9770-vetrne-podminky-v-ceske-republice-ve-vysce-10-m-nad-povrchem-i

Hanslian, D., Hošek, J., Chládová, Z., & Pop, L. (2013). Větrné podmínky v České republice ve výšce 10 m nad povrchem II. *TZB-info*, 22.4.2013. http://oze.tzb-info.cz/vetrna-energie/9770-vetrne-podminky-v-ceske-republice-ve-vysce-10-m-nad-povrchem-ii

Hanslian, D., Chládová, Z., Pop, L., & Hošek, J. (2014). Větrná mapa České republiky ve výšce 100 m nad povrchem. *Meteorologické zprávy*. [accepted]

Hanslian, D., & Hošek, J. Combining the WAsP model and the VAS 3D interpolation method to produce a high-resolution wind resource map for the Czech Republic. *Wind Energy*. [under review]

Pop, L., Hošek, J., & **Hanslian, D.** Mapping of extreme wind speed for landscape modelling of the Bohemian Forest, Czech Republic. *Natural Hazards and Earth System Sciences*. [under review]

(selected other results)

Hanslian, D., Hošek, J., Chládová, Z., Pop, L., Svoboda, J., & Štekl, J. (2007): Určení technického potenciálu větrné energie na území České republiky. <Neveřejná výzkumná zpráva> Ústav fyziky atmosféry AV ČR, Praha, 78p.

Sokol, Z., Štekl, J., **Hanslian, D.**, Hošek, J., & Jež, J. (2007): Časová a prostorová variabilita rychlostí větru se zřetelem na činnost větrných elektráren. <Neveřejná výzkumná zpráva> Ústav fyziky atmosféry AV ČR, Praha, 60p.

Hanslian, D., Hošek, J., & Štekl, J. (2008). *Odhad realizovatelného potenciálu větrné energie na území České republiky*. Ústav fyziky atmosféry AV ČR, Praha, 32p. http://www.ufa.cas.cz/vetrna-energie/doc/potencial_ufa.pdf.

Hanslian, D. & Pop, L. (2008). The technical potential of wind energy and a new wind atlas of the Czech Republic. In: *Proceedings of the European wind energy conference*.

Hanslian, D. (2008). Two measure-correlate-predict methods and their performance. In: *Proceedings of the European wind energy conference*.

Hošek, J., & **Hanslian, D.** (2010): Území s dostatečným větrným potenciálem pro výstavbu větrných elektráren. <Specializovaná mapa s odborným obsahem.> http://geoportal.gov.cz

Hošek, J., **Hanslian, D.**, Svoboda, J., Chládová, Z., & Pop, L. (2010): Mapa průměrné rychlosti větru ve 100 m nad zemským povrchem. <Specializovaná mapa s odborným obsahem.> http://geoportal.gov.cz

Hanslian, D., & Hošek, J. (2012): Aktualizovaný odhad realizovatelného potenciálu větrné energie z perspektivy roku 2012. Ústav fyziky atmosféry AV ČR, Praha, 23p.